Biosensors and Bioelectronics 157 (2020) 112159

Contents lists available at ScienceDirect

Biosensors and Bioelectronics

journal homepage: http://www.elsevier.com/locate/bios

Mass spectrometric biosensing: Quantitation of multiplex enzymes using single mass probe and fluorous affinity chip

Nan Feng, Junjie Hu, Qiulin Ma, Huangxian Ju *

State Key Laboratory of Analytical Chemistry for Life Science, School of Chemistry and Chemical Engineering, Nanjing University, Nanjing, 210023, PR China

ARTICLE INFO

Keywords:
Mass spectrometric biosensing
Mass probe
MALDI-MS quantitation
Fluorous affinity chip
Multiplex enzyme activities

ABSTRACT

This work presents a concept of "mass spectrometric biosensing" by using a chip to recognize the targets and mass spectrometry to detect the signals switched by the recognition. The chip is prepared on an ITO slide with a hydrophobic fluorous-tag monolayer to self-assemble the mixture of mass probe and fluorous-tagged cysteine as a spacer through fluorous affinity interaction. The presence of spacer provides suitable conditions for recognition reactions on the chip. By designing a single mass probe as the peptide substrates of corresponding target enzymes, a novel quantitative strategy based on the ratio of signal intensities of different species on the chip is developed for MALDI-MS assay of multiplex enzyme activities. Using caspase-3 and protein kinase A as targets, the reactions with designed mass probe produce three mass shifts to act as two "fingerprint" patterns for obtaining the dual enzyme activities. The proposed biosensing method shows the detectable ranges from 0.05 to 50 μU μL^{-1} and 0.4–40 μU μL^{-1} with correlation coefficients of 0.990 and 0.989 for PKA and caspase-3, respectively. The biosensing application has been demonstrated by monitoring these enzymes in cell lysates upon anti-cancer drug treatment, indicating the prospect of the novel biosensing protocol in biomedical study.

1. Introduction

Matrix-assisted laser desorption/ionization mass spectrometry (MALDI-MS) has been used as a powerful tool for assessment of enzyme activities due to its label-free and high-throughput properties (Liesener and Karst, 2005; Hu et al., 2015). However, since the component of biological samples is particularly complex, this technology often suffers from tedious sample preparation, such as separation and desalting protocols (Gu et al., 2006; Percy et al., 2013; Onagi et al., 2017; Meng et al., 2018). To simplify the preparation, different self-assembled monolayers have been designed for analysis of enzymes (Min et al., 2004; Ban et al., 2012; Kightlinger et al., 2018), protein interactions (Yeo et al., 2005; O'Kane and Mrksich, 2017), and organic reactions (Montavon et al., 2012). The monolayers can be prepared by hydrophobic interaction between alkyl chains on a gold chip (Sanchez-Ruiz et al., 2011) or ITO glass slide (Beloqui et al., 2013). Upon the interaction of the monolayers with the analytes in complex sample, the chip or ITO slide can be directly used for collecting the changes of mass/charge (m/z) ratios or/and their intensities as detectable signals, which matches completely the switch character of biosensing. Inspired by this character, here a novel concept of "mass spectrometric biosensing" was proposed by introducing specific interaction on chip interface for recognition of target analytes. As a proof-of-concept, a biosensing chip was prepared through fluorous affinity interaction to form an enzyme-specific recognition interface.

The fluorine-fluorine interaction is generally rather weak due to the low polarizability of fluorine atom, thus it is not used significantly in the building of supramolecular structure (Legon, 2010). However, the perfluorination of alkyl chains can greatly enhance the interaction, and has been used to construct the perfluorinated self-assembled monolayer (Baker et al., 2012). Moreover, the perfluorinated chain is chemically inert and compatible with a wide range of functional groups (Nicholson et al., 2007), and is also rarely found in biological system such as cell lysates (Kim et al., 2011; Yang et al., 2016). Thus it has been used as an affinity fluorous tag for preparation of microarray (Nicholson et al., 2007; Vegas et al., 2007) and labelling of carbohydrate (Ko et al., 2005; Northen et al., 2008). The "soft" immobilization via fluorous-phase interactions can avoid the interference from complex biological samples through a surface washing step, and allows efficient desorption/ionization of tagged carbohydrates for mass spectrometry-based enzyme activity assay (Northen et al., 2008). This work designed a single mass probe for multiplex quantitative assay of enzyme activities by using

* Corresponding author.
E-mail address: hxju@nju.edu.cn (H. Ju).

https://doi.org/10.1016/j.bios.2020.112159
Received 31 December 2019; Received in revised form 2 March 2020; Accepted 17 March 2020
Available online 20 March 2020

perfluorinated alkyl chain to tag a peptide chain, which was simply performed through click reaction between thiol and maleimide groups (Luo et al., 2013). The linkage of fluorous tag increased the molecular weight of enzymatic products for avoiding the interference caused by matrix (Ma et al., 2013). Considering the steric effect of the densely packed fluorous-tagged peptide (FTP) monolayer, which is not facile for enzyme to access to substrate, fluorous-tagged cysteine as a spacer was also co-assembled on the biosensing chip (Fig. 1A).

MALDI MS quantitation is usually difficult due to the presence of "sweet spot" effect. By chemically tagging the cysteine residues of peptides, our previous work developed an internal standard method for MALDI MS quantitation (Ma et al., 2014). Prior to the signal collection, the target in both standard and sample solutions was firstly tagged with benzoquinone and methyl-p-benzoquinone, respectively, and the resulting solutions were then mixed to perform the MS quantitation. To avoid the operation of sample preparation, we further designed a peptide microarray to develop a mass imaging-based quantitation technique (Hu et al., 2016). The sample could be directly dropped on the microarray spots for recognition of target analytes. However, the MALDI-MS scan for image acquisition was time-consuming. To solve this limitation, this work used caspase-3 and protein kinase A (PKA) as targets to design the single mass probe, and found the "fingerprint" pattern of corresponding enzyme from the MALDI-MS spectrum. The "fingerprint" pattern was novel *m/z* signals upon the enzyme recognition on the biosensing chip. For caspase-3 and PKA recognition, the patterns included decreased and increased *m/z*, and a third mass shift due to the hydrolysis and phosphorylation of the mass probe (Fig. 1A). The quantitative signal for each enzyme could be obtained from the intensity ratio of related products to all *m/z* peaks. Based on the "mass spectrometric biosensing" concept, the quantitation of multiplex enzyme activities became simpler and more effective. The proposed strategy could be conveniently used for quantitatively monitoring intracellular caspase-3 and PKA activities upon the treatment of anticancer drug, indicating the promising application of the novel biosensing platform in quantitation of intracellular kinases and proteases for regulation of cell apoptosis (López-Otín and Hunter, 2010) and biomedical study.

2. Experimental

2.1. Materials and reagents

ITO glass slides (75 mm × 25 mm × 1.1 mm) were purchased from Huanan Xiangcheng Technology Co., Ltd. (Shenzhen, China). Cyano-4-hydroxy-cinnamic acid (CHCA, ≥99.0%), 1,4-dithiothreitol (DTT), trifluoroacetic acid (TFA, ≥99.0%), N-(4,4,5,5,6,6,7,7,8,8,9,9,10,10,11,11,11-heptadecafluoroundecyl)maleimide (≥95%), 1H,1H,2H,2H-perfluorooctyltriethoxysilane (≥98%), ethylenediaminetetraacetic acid (EDTA, ≥99%), caspase 3 human (≥90%, SDS-PAGE, ≥1 units mg^{-1} protein),[a] adenosine 5′-triphosphate (ATP) disodium salt hydrate, H-89 dihydrochloride hydrate (≥98%), forskolin (≥98%), 3-isobutyl-1-methylxanthine (IBMX, ≥99%), acetyl-DEVD-CHO (≥95%) and acetyl-LDESD-CHO (≥94%) were obtained from Sigma-Aldrich (U.S.A.). The

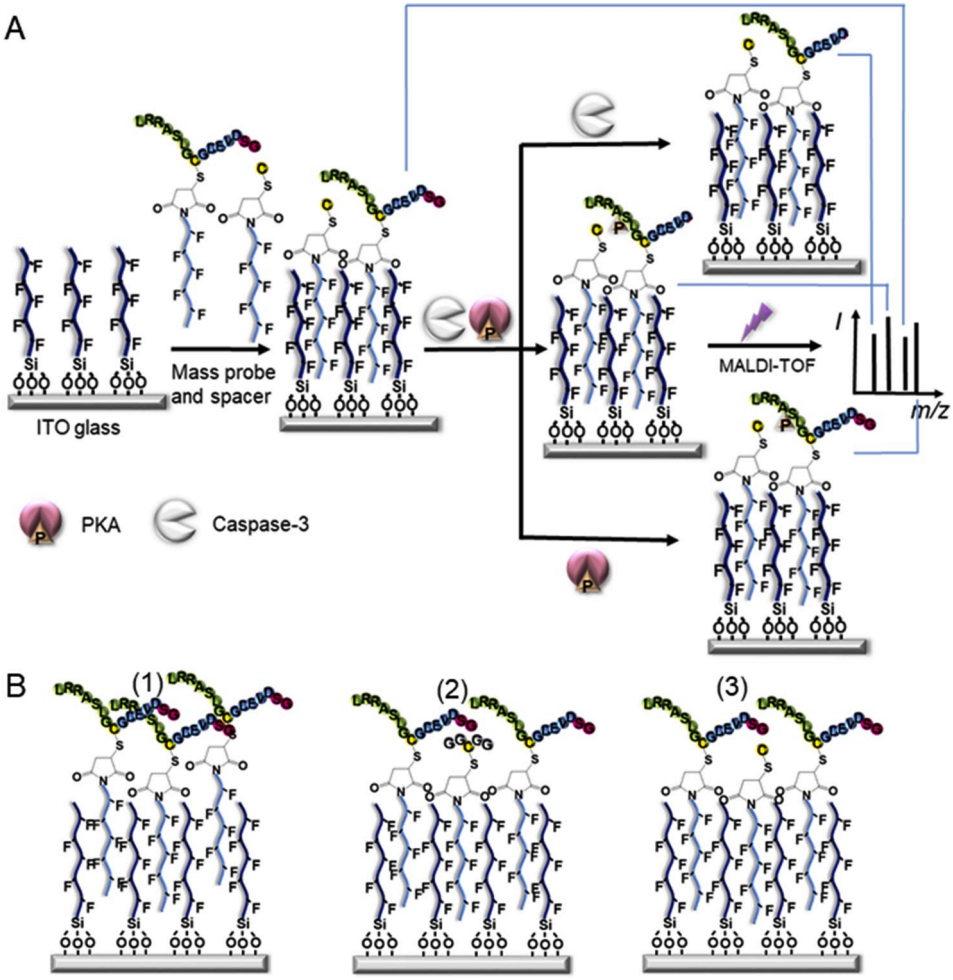

Fig. 1. (A) Assembly of FTP on fluorooctyl ITO slide through fluorous affinity interaction and enzymatic reactions for MALDI-TOF MS quantitation of dual enzyme activities. (B) Mass spectrometric biosensing chips prepared with FTP (1) and the mixture of FTP and fluorous tagged acetyl-GGCGG-NH_2 (2) or fluorous tagged cysteine (3) as spacer on fluorooctyl slide.

cAMP-dependent protein kinase A (PKA, catalytic subunit) was purchased from New England BioLabs (Beverly, MA, U.S.A.). 5(6)-Carboxyfluorescein, succinimidyl ester (5(6)-FAM-NHS, ≥ 90%) was obtained from J&K Chemical Ltd. (Beijing, China). Acetonitrile, methanol, acetone, ethanol, tetrahydrofuran (THF), hydrogen peroxide (H_2O_2), ammonium hydroxide ($NH_3•H_2O$), ammonium acetate (NH_4Ac), sodium chloride (NaCl), magnesium chloride ($MgCl_2$), dichloromethane (DCM) and cysteine were purchased from Nanjing Chemical Reagent Co., Ltd. (Nanjing, China). 2,5-Dihydroxybenzoic acid (DHB, ≥ 98%) was obtained from Heowns Biochem Technologies Co., Ltd. (Tianjin, China). Doxorubicin hydrochloride (DOX) was purchased from Aladdin Industrial Co., Ltd. (Shanghai, China). Peptides were synthesized and purified by Sangon Biotech (Shanghai, China) with purity greater than 95.0%. One step animal cell active protein extraction kit was supplied by Sangon (Shanghai, China). Phosphate buffer saline (PBS) was obtained from Jiangsu KeyGEN BioTECH Co., Ltd. (Nanjing, China). All these reagents were used as received without further purification. Ultrapure water (≥18.2 MΩ, Milli-Q, Millipore) was used through the experiment.

[a]One unit can cleave 1.0 μmole of N-acetyl-Asp-Glu-Val-Asp-pNA per min at pH 7.4 at 25 °C.

2.2. Apparatus

MALDI-TOF mass spectrometric experiments were performed on a 4800 *plus* MALDI TOF/TOF analyzer (AB sciex, U.S.A.) with Nd:YAG laser at 355 nm, a repetition rate of 200 Hz, and an acceleration voltage of 20 kV. The data analysis was performed with a Data Explorer™ Software from AB Sciex (U.S.A.). The MALDI-MS imaging was operated in a positive linear mode in the range of *m/z* 1500–2500 with the image acquisition software 4800 Imaging (Novartis, Basel, Switzerland), which was available through the MALDI-MSI web site (http://www.maldi-msi.org). 200 μm × 200 μm was used as the acquisition step size. All data were processed on BioMap (Novartis, Basel, Switzerland), which could also be downloaded from the same web site.

The contact angles were measured with an OCA30 contact angle system (Dataphysic Instruments GmbH, Germany) using droplets of 1.0 μL ultrapure water at room temperature (RT). X-ray photoelectron spectroscopy (XPS) was carried out with PHI 5000 VersaProbe (ULVAC-PHI, Japan). SEM images were gained on a JEM-7800 scanning electron microscope (JEOL, Japan) equipped with an energy dispersive X-ray spectroscopic facility to obtain EDS mapping. The fluorescence image of chip was taken with a Biochip Analysis System (Capitalbio, China). Cell numbers were determined with a Petroff-Hausser cell counter (U.S.A.).

2.3. Surface modification of indium tin oxide (ITO) slides

According to our previous report (Hu et al., 2016), the ITO slides were firstly ultrasonically cleaned in acetone, ethanol and water for 20 min, respectively, followed with immersion in basic piranha solution (the mixture of 60 mL H_2O, 22.5 mL H_2O_2, and 22.5 mL $NH_3•H_2O$) at 60 °C for 1 h. After these slides were washed twice with water, purged with N_2, and immersed in 0.2% 1H,1H,2H,2H-perfluorooctyltriethoxysilane in DCM overnight at RT, the obtained fluorooctyl slides were washed twice with DCM, dried with N_2, and stored under vacuum at RT until use. The Au/ITO (5 nm chrome followed by 50 nm gold) slide was fabricated as control with electron beam evaporation technique (DE Tec. Ltd., U.S.A.).

2.4. Synthesis of fluorous-tagged peptide conjugate (FTP)

Acetyl-LRRASLGCGDEVDSG-NH_2 (M_w = 1575.72) was used as the substrate for both caspase-3 and PKA (Hu et al., 2016; Zhang et al., 2015). 2 mM of the cysteine-containing peptide in 0.5 M NH_4Ac solution was firstly mixed with 2 mM fluorous tag dissolved in tetrahydrofuran at the same volume for coupling N-(4,4,5,5,6,6,7,7,8,8,9,9,10,10,11,11,11-heptadecafluoroundecyl)maleimide as fluorous tag to the peptide substrate. The click reaction between the –SH group of cysteine and maleimide group of fluorous tag was carried out with gentle shaking at RT for 2 h (Han et al., 2013). The obtained FTP was stored at −20 °C for further use without separation or purification. For the optimization of FTP density on the assay chip, acetyl-GGCGG-NH_2 or cysteine labeled fluorous tag was synthesized with the same procedure.

2.5. Fabrication of mass spectrometric biosensing chips (MSC)

Using caspase-3 and PKA as enzymatic model for simultaneous assay of multiplex enzyme activities, the FTP was self-assembled on the fluorooctyl slide obtained above via fluorous-fluorous interaction, which was performed by spotting 0.25 μL of the mixture of FTP and fluorous tagged cysteine at a ratio of 1:6 on the slide at 4 °C overnight. The resulting MSC was washed thrice with acetonitrile/water (3:7), and dried with N_2. As control, 0.25 μL of FTP or the mixture of FTP and fluorous tagged acetyl-GGCGG-NH_2 at a ratio of 1:4 was spotted on the fluorooctyl slide.

To examine the morphology and distribution of the FTP spots with fluorescence imaging technique, the substrate was mixed with 1 mM 5(6)-FAM-NHS in PBS (pH 7.5) at the same volume for 4 h at RT to label the terminal amine.

2.6. MALDI-TOF MS analysis

For analysis of peptides and peptide conjugates, 1 μL of the peptide solution (1 mM) was spotted on a 384-well Opti-TOF stainless steel MALDI plate (AB Sciex, U.S.A.) and left to dry. Thereafter, 1 μL of 50 mg mL^{-1} DHB in the mixture of methanol and water (1:1, v/v) was induced as matrix. The MALDI-MS spectra were automatically acquired using a positive linear or reflector mode with a fixed laser intensity. For each spectrum, 200 shots from different positions of the target spot (automatic mode) were collected. The MS/MS spectrum was obtained using a positive MS/MS mode with fixed laser intensity in the range of *m/z* 200–2000. Fragmentation was performed using the CID mode with an assigned precursor mass window.

2.7. Dual-enzyme activity assay

To acquire the information of dual-enzyme activity, 1 μL solution of PKA and caspase-3, prepared with assay buffer containing 50 mM Tris-HCl, 10 mM $MgCl_2$, 0.1 mM EDTA, 2 mM DTT and 200 μM ATP, was dropped on each specific spot of MSC and incubated at 37 °C for an optimal reaction time of 40 min, which was optimized at 25 μU $μL^{-1}$ PKA and 10 μU $μL^{-1}$ caspase-3. The enzymatic reactions were stopped by rinsing the MSC twice with ultrapure water, and the MALDI-MS analysis was performed by dropping 0.25 μL of 50 mg mL^{-1} DHB on the spot as the matrix, which was dissolved in the mixture of methanol and water (1:1, v/v). The prepared mass spectrometric biosensing chip was compatible to the mass spectrometer. It could be stuck to the MALDI plate to locate the spots on chip by the logical x and y coordinates for MS measurements.

To get inhibition curves, 20 μU $μL^{-1}$ caspase-3 was pre-mixed with its inhibitor acetyl-DEVD-CHO (0.1 nM−1.0 mM) or acetyl-LDESD-CHO (0.1 nM−1.0 mM), and 20 μU $μL^{-1}$ PKA was pre-mixed with its inhibitor H-89 (0.1 nM−2.0 mM) in assay buffer for 30 min, which were then added onto the MSC to react for 40 min at 37 °C to perform the MALDI-MS analysis.

2.8. Cell culture and lysis

Human breast cancer MCF-7 cells and cervical cancer Hela cells were obtained from KeyGEN Biotech Co., Ltd. (Nanjing, China). They were firstly seeded in 6-well plates (Corning, NY, U.S.A.) at a density of 2 × 10^5/mL, and cultured overnight in RPMI 1640 or DMEM medium (KeyGEN, Nanjing, China) in a humidified atmosphere containing 5%

CO_2 at 37 °C, respectively. Both media contained 10% fetal bovine serum (FBS), 100 μg mL^{-1} penicillin, and 100 U mL^{-1} streptomycin. These cells were treated with DOX from 0.05 to 5 μg mL^{-1} in FBS-contained medium for 19.5 h and then DOX at the same concentration in 2.0 mL FBS-free medium for 4 h. Afterward, 20 μL of the mixture of 5.0 mM Forskolin and 10 mM IBMX in DMSO was added to the medium to activate PKA for 30 min (Zhang et al., 2015).

The cell lysis was performed with commercial protein extraction solution (One Step Animal Cell Active Protein Extraction Kit, Sangon). The lysates were centrifuged at 14000 rpm at 4 °C for 10 min, and then the supernatants were collected to ultrafilter with 50 mM Tris-HCl, 10 mM $MgCl_2$, 0.1 mM EDTA, 2 mM DTT and 200 μM ATP to a final volume of 100 μL for enzyme detection.

2.9. Cell apoptosis experiments

The MCF-7 and Hela cells treated with 0 (as controls), 0.5 or 5 μg mL^{-1} DOX for 24 h were harvested by trypsin (KeyGEN Biotech Co., Ltd., Nanjing, China) and centrifuged. After the cells were dispersed in binding buffer, they were stained with the mixture of 5.0 μL Annexin V-APC and 5.0 μL 7-AAD (KeyGEN Biotech Co., Ltd., Nanjing, China) in dark for 15 min at RT. The cell apoptosis was analyzed on a Cytomics FC500 flow cytometer (BeckmanCoulter, U.S.A.) over FL3 (7-AAD) and FL4 (Annexin V-APC) channels.

3. Results and discussion

3.1. Fabrication of mass spectrometric biosensing chip (MSC)

On account of the conductivity and compatibility of commercial ITO slide to mass spectrometer, the mass spectrometric biosensing chip (MSC) was constructed by self-assembling the mass probe FTP and the spacer fluorous-tagged cysteine on a fluorooctyl ITO slide. Upon the modification of ITO slide with 1H,1H,2H,2H-perfluorooctyltriethoxysilane, it showed a contact angle change from 11.5° to 107.3° (Fig. S1), indicating the presence of hydrophobic perfluorinated chain, which led to the F1s peak at 685 eV in XPS spectrum (Fig. S2) and the uniformly fluorous distribution in EDS mapping (Fig. S3) of the fluorooctyl ITO slide.

The FTP synthesized with the substrate peptide acetyl-LRRASLGCGDEVDSG-NH_2 and fluorous-tagged cysteine were confirmed by the MALDI MS and MS/MS spectra (Figs. S4 and S5), respectively. The MS/MS spectrum of FTP showed its two components. After assembling FTP on the hydrophobic surface through fluorine-fluorine interaction, the surface showed the peak of FTP at *m/z* 2132.4 (Fig. S6). The uniformly assembly of FTP on the hydrophobic surface was verified with the fluorescence image by coupling fluorous-tagged LRRASLGCG-DEVDSG with FAM (Fig. S7). In order to confirm the fluorine-fluorine interaction during the self-assembly process, the ITO and fluorooctyl ITO slides were treated with FTP and substrate peptide to record the mass spectra, respectively, which did not show any signal (Fig. S8). Moreover, the assembly through fluorine-fluorine interaction showed much better performance of desorption/ionization than that through Au–S interaction on Au/ITO surface due to the presence of cysteine residues in the substrate peptide (Fig. S9).

To optimize the spacer and the density of the mass probe FTP for surface enzymatic recognition, fluorous-tagged acetyl-GGCGG-NH_2 (Fig. S10) and fluorous-tagged cysteine were respectively mixed with FTP at different ratios for the preparation of MSCs (Fig. 1B), which showed the characteristic MS peaks of spacer and FTP (Fig. 2A and B). After incubating the MSCs with caspase-3 and PKA for 40 min, respectively, their mass spectra showed the signals of FTP and the products at *m/z* 1990 and 2213 (Fig. S11). These product peaks resulted from the caspase-3 catalyzed cleavage of the substrate peptide at the C-terminal of Asp residue, and the PKA catalyzed phosphorylation at the location of serine of the mass probe. The cleavage led to a mass decrease of 142.5 Da

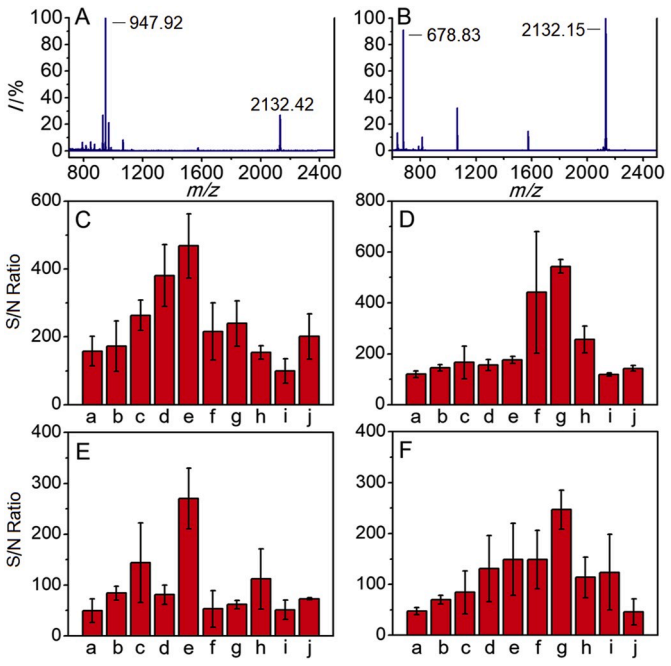

Fig. 2. (A) Mass spectra of MSCs prepared by assembly of FTP and (A) fluorous tagged acetyl-GGCGG-NH_2 or (B) fluorous tagged cysteine on fluorooctyl slide, and FTP density optimization at MSC prepared with FTP (a) or the mixture of (C,E) fluorous-tagged acetyl-GGCGG-NH_2 or (D,F) fluorous-tagged cysteine with FTP at the molar ratio of 1:1, 2:1, 3:1, 4:1, 5:1, 6:1, 7:1, 8:1 and 9:1 (from b-j) through the S/N ratio of phosphorylation product in 10 μU μL^{-1} PKA (C,D) and cleavage product in 1 μU μL^{-1} caspase-3 (E,F) for 40 min.

for dipeptide Ser–Gly–NH_2 segment, while the phosphorylation increased a mass of 80 Da for a phosphate group. After enzymatic reactions, the MSCs prepared with fluorous-tagged acetyl-GGCGG-NH_2 as spacer showed the maximum S/N ratios of the products at the molar ratio of 4:1 (Fig. 2C and E), while the maximum S/N ratios for fluorous-tagged cysteine spacer occurred at the molar ratio of 6:1 (Fig. 2D and F). At the optimal molar ratios, the fluorous-tagged cysteine spacer showed 1.2 times higher S/N ratio than fluorous-tagged acetyl-GGCGG-NH_2 for PKA, and slightly lower S/N ratio for caspase-3. Thus the spacer was further optimized with the enzymatic reaction efficiency, which was calculated with $[I_{pro}/(I_{pro} + I_{sub})] \times 100\%$, where I_{pro} and I_{sub} are the peak intensity of the product and substrate after enzymatic reaction, respectively (Hu et al., 2016). As shown in Fig. S12, the enzymatic reaction efficiency, which could be considered as the enzymatic activity, increased almost linearly with the increasing logarithm value of enzyme concentration (μU μL^{-1}, strictly calculated according to the instructions of commercial enzymes) and the presence of spacer improved obviously the efficiency and widened the detectable range. Moreover, the MSC prepared with fluorous-tagged cysteine as spacer showed better performance for both PKA and caspase-3. Thus this work used the mixture of 0.1 mM FTP and 0.6 mM fluorous-tagged cysteine for preparation of the MSC, which showed neat arrangement and uniform distribution of the spots after DHB as the matrix was dropped on the specific spots (Fig. S13). Through converting the signal of different enzymatic reactions into corresponding *m/z* and the intensities, the mass spectrometric biosensing could be achieved.

3.2. Quantitation of multiplex enzymes

When the optimal MSC was incubated with the mixture of caspase-3 and PKA, its MS images showed all the signals of FTP at *m/z* 2132.4, cleavage product at *m/z* 1990 and phosphorylation product at *m/z* 2213, and a new peak occurred at *m/z* 2070, which resulted from the phosphated hydrolysis product (Fig. 3). The specificity of the MSC

towards the recognition of target enzymes was further verified by assembling a peptide without the reaction site for both PKA and caspase-3 on the fluorooctyl ITO slides, which did not show any change of MALDI mass spectra after incubated with these enzymes and their mixture (Fig. S14). Therefore the disparate mass shifts excluded the false positive/interferences between the dual enzymes.

Taking PKA and caspase-3 as model targets, the recognition of dual target enzymes to the MSC produced three mass shifts (Fig. 4A), which could be defined as two "fingerprints" for PKA and caspase-3, respectively, due to the phosphorylation and hydrolysis of the designed peptide. The intensity ratios of related product peaks to all peaks, i.e. $[(I_{2213} + I_{2070})/(I_{1990} + I_{2070} + I_{2133} + I_{2213})] \times 100\%$ and $[(I_{1990} + I_{2070})/(I_{1990} + I_{2070} + I_{2133} + I_{2213})] \times 100\%$, could be considered as the enzymatic reaction efficiency of PKA and caspase-3, respectively, where I_{2213} stands for the product of PKA, I_{1990} stands for the product of caspase-3, I_{2070} is the peak intensity of phosphated hydrolysis product in the presence of dual enzymes, and I_{2133} the peak intensity of FTP. Very interestingly, the ratio showed linear correlation to the logarithm of enzyme concentration of PKA or caspase-3 (Fig. 4B and C), leading to a quantitative method for simultaneous activity analysis of dual target enzymes. At an optimal incubation time of 40 min for recognition of two target enzymes (Fig. S15), the biosensing method showed a detectable range from 0.05 to 50 μU μL^{-1} and 0.4–40 μU μL^{-1} with a correlation coefficient of 0.990 and 0.989 for PKA and caspase-3, respectively. The sensitivities were calculated to be 19.5 μL μU^{-1} and 36.0 μL μU^{-1} for PKA and caspase-3, respectively, illustrating good sensitivity of the proposed method. According to the principle of 3σ, the limits of detection were 0.024 μU μL^{-1} and 0.40 μU μL^{-1}. In order to examine the reproducibility, the method was carried out at 10 μU μL^{-1} PKA in the presence of 20 μU μL^{-1} caspase-3, and 10 μU μL^{-1} caspase-3 in the presence of 20 μU μL^{-1} PKA for 6 times respectively, and the RSDs of enzymatic reaction efficiency were detected to be 1.37% for PKA and 2.34% for caspase-3, reflecting a good reproducibility of the proposed chip. The detection procedure demonstrated that the mass spectrometric biosensing chip could be used to detect multiplex target enzymes and was much simpler and faster than previously developed internal standard method (Ma et al., 2014) and imaging technique (Hu et al., 2016).

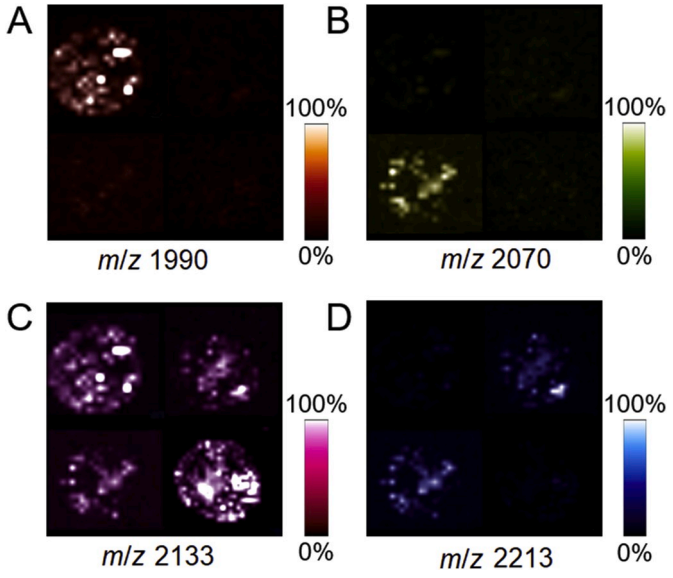

Fig. 3. MS images of MSCs after reaction with caspase-3 (upper left spot), PKA (upper right spot), dual enzymes (lower left spot) in assay buffer, and assay buffer (lower right spot) for color-coded *m/z* of (A) 1990 (B) 2070 (C) 2133 (D) 2213.

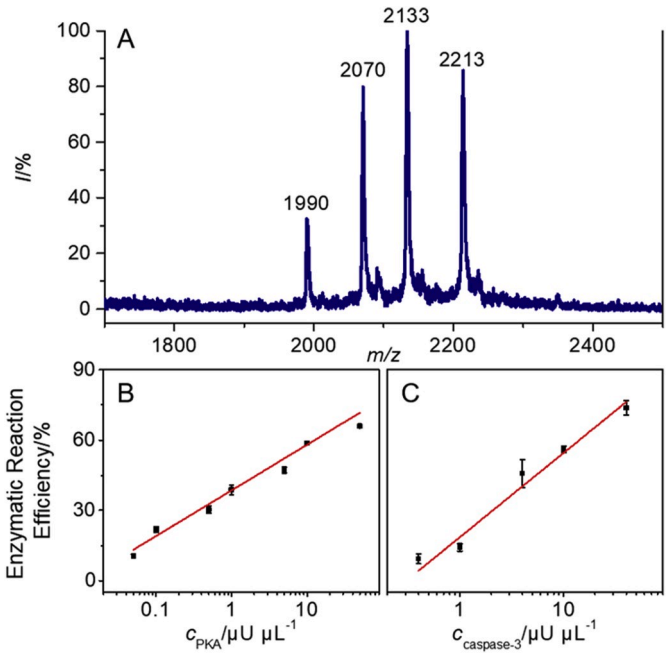

Fig. 4. (A) Mass spectrum of MSC after enzymatic reactions with 10 μU μL^{-1} PKA and caspase-3, and plots of enzymatic reaction efficiency vs (B) PKA concentration in the presence of 20 μU μL^{-1} caspase-3 and (C) caspase-3 concentration in the presence of 20 μU μL^{-1} PKA.

3.3. Analysis of enzymatic inhibitors

The proposed biosensing method was firstly used to evaluate the effect of inhibitor on enzyme activity. Using H-89 as an inhibitor of PKA, the IC_{50} was detected to be 31 nM (Fig. S16A), close to previously reported 39.5 nM (Bai et al., 2013) and 23.1 nM (Zhou et al., 2014). The inhibitor acetyl-DEVD-CHO for caspase-3 showed an IC_{50} value of 12 nM (Fig. S16B), which slightly lower than the reported values of 18 and 21 nM (Vickers et al., 2013a,b). These results indicated the feasibility of the proposed biosensing strategy for screening the effective inhibitors. For example, the IC_{50} of acetyl-LDESD-CHO for caspase-3 was measured to be 0.76 μM (Fig. S16C), showing weaker inhibition.

3.4. Monitoring of multiplex enzymes in cell lysates

The designed single mass probe was further used to monitor the activity of these enzymes in cell lysates during anti-cancer drug treatment. Both human breast cancer MCF-7 cells and cervical cancer Hela cells were selected as the models. They were incubated with doxorubicin (DOX), a widespread anti-tumor drug through activating caspase family to induct cell apoptosis (Xu et al., 2012) in FBS-contained medium, and then treated with DOX and its mixture with Forskolin and 3-isobutyl-1--methylxanthine in FBS-free medium to activate PKA through increasing intracellular cAMP (Minotti et al., 2004). These cells were lysed with one step animal cell active protein extraction kit. After the cell debris (Fig. S17) were removed by centrifugation, 1 μL of lysates were directly dropped on the MSC spots for enzymatic reactions and MALDI-MS analysis. For Hela cells, the maximum activity of PKA occurred at 0.1 μg mL^{-1} DOX, while caspase-3 showed continuous increase with the increasing DOX concentration (Fig. 5A). The treated MCF-7 cells showed only PKA activity, since functional caspase-3 in MCF-7 cells lost (Jänicke, 2009; Jänicke et al., 2001), suggesting different apoptosis path of MCF-7 cells from Hela cells (Yuan et al., 2017). At high dose of DOX, both cells showed decreased PKA activity, indicating the effect of caspase-3 on PKA (López-Otín and Hunter, 2010), possibly due to the cell apoptosis prior to PKA activation. The cell apoptosis was validated with flow cytometry using Annexin V-APC/7-AAD apoptotic kit. 0.5 and

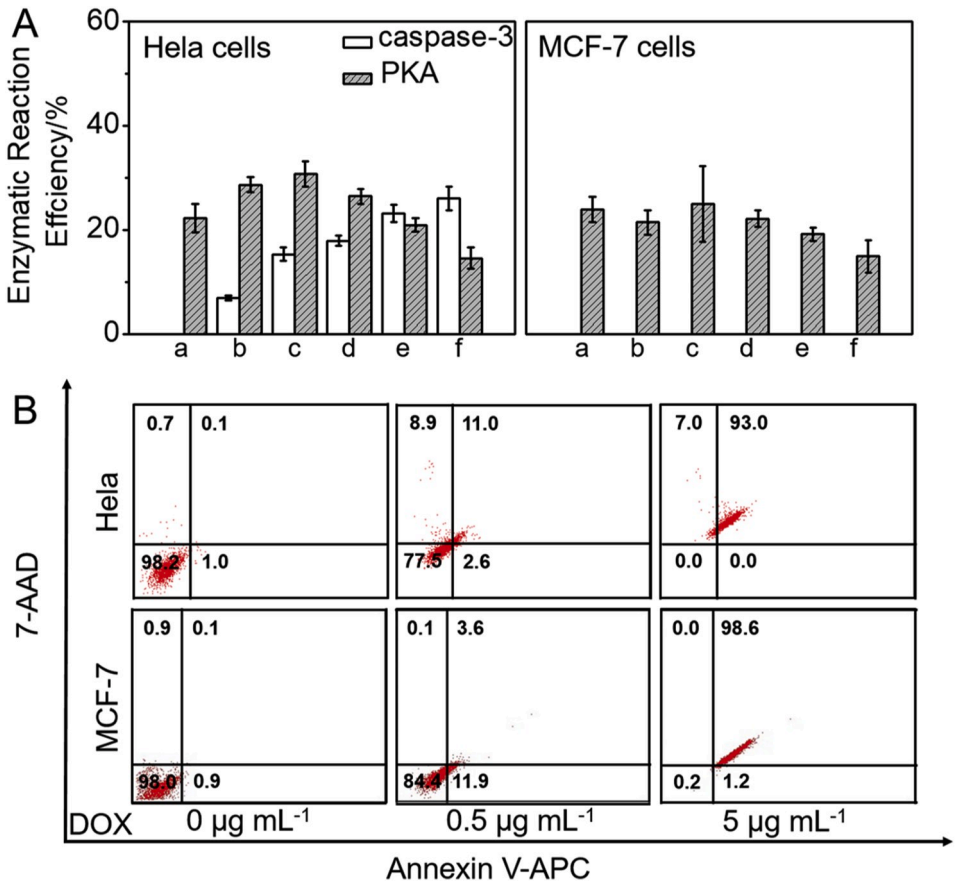

Fig. 5. (A) Enzymatic reaction efficiency of PKA and caspase-3 in cell lysates collected from Hela and MCF-7 cells after treated with 0, 0.05, 0.1, 0.5, 1.0 and 5.0 μg mL^{-1} DOX (from a to f) and then their mixture with Forskolin and 3-isobutyl-1-methylxanthine, and (B) flow cytometric analysis of cells treated with DOX for 24 h using Annexin V-APC/7-AAD apoptosis detection kit.·

5 μg mL^{-1} DOX treated MCF-7 cells showed the apoptosis rate of 15.5% and 99.8%, respectively, and the apoptosis rate of Hela cells with the same treatment were 13.6% and 93% (Fig. 5B).

4. Conclusion

This work demonstrates the concept of "mass spectrometric biosensing" by introducing specific interaction on chip interface for recognition of target analytes, and the special "fingerprint" patterns for convenient analysis of multiplex enzymes with a designed single mass probe. A novel method for fabrication of the chip is proposed by tagging the peptide substrate with perfluorinated alkyl chain for hydrophobic assembly through fluorine-fluorine interaction. The quick MALDI-MS quantitation of enzyme activity has been achieved without internal standard with acceptable linear correlation, good sensitivity and reproducibility, and used for evaluation of enzyme inhibitors and quantitative monitoring of intracellular caspase-3 and PKA activities upon the treatment of anticancer drug. The novel biosensing strategy can be extended for quantitation of other targets by introducing different signal switches. This protocol possesses potential application in revealing intracellular pathways and related biological processes.

Declaration of competing interest

The authors declare that they have not known competing financial interests or personal relationships that could have appeared to influence the work reported in this paper.

CRediT authorship contribution statement

Nan Feng: Conceptualization, Investigation, Writing - original draft, Methodology. **Junjie Hu:** Conceptualization, Investigation. **Qiulin Ma:** Investigation. **Huangxian Ju:** Conceptualization, Project administration, Funding acquisition, Writing - review & editing.

Acknowledgements

We gratefully acknowledge the National Natural Science Foundation of China (21635005, 21827812, 21890741, 21904049) and National Key Research and Development Program of China (2018YFC1004704).

Appendix A. Supplementary data

Supplementary data to this article can be found online at https://doi.org/10.1016/j.bios.2020.112159.

References

Bai, J., Zhao, Y.J., Wang, Z.B., Liu, C.H., Wang, Y.C., Li, Z.P., 2013. Anal. Chem. 85, 4813–4821.
Baker, R.J., Colavita, P.E., Murphy, D.M., Platts, J.A., Wallis, J.D., 2012. J. Phys. Chem. A 116, 1435–1444.
Ban, L., Pettit, N., Li, L., Stuparu, A.D., Cai, L., Chen, W.L., Guan, W.Y., Han, W.Q., Wang, P.G., Mrksich, M., 2012. Nat. Chem. Biol. 8, 769–773.
Beloqui, A., Calvo, J., Serna, S., Yan, S., Wilson, I.B.H., Martin-Lomas, M., Reichardt, N. C., 2013. Angew. Chem. Int. Ed. 52, 7477–7481.
Gu, X., Deng, C.H., Yan, G.Q., Zhang, X.M., 2006. J. Proteome Res. 5, 3186–3196.
Han, G.J., Zhang, S.C., Xing, Z., Zhang, X.R., 2013. Angew. Chem. Int. Ed. 52, 1466–1471.
Hu, J.J., Liu, F., Ju, H.X., 2015. Anal. Chem. 87, 4409–4414.

Hu, J.J., Liu, F., Ju, H.X., 2016. Angew. Chem. Int. Ed. 55, 6667–6670.
Jänicke, R.U., 2009. Breast Canc. Res. Treat. 117, 219–221.
Jänicke, R.U., Engels, I.H., Dunkern, T., Kaina, B., Schulze-Osthoff, K., Porter, A.G., 2001. Oncogene 20, 5043–5053.
Kightlinger, W., Lin, L., Rosztoczy, M., Li, W.H., DeLisa, M.P., Mrksich, M., Jewett, M.C., 2018. Nat. Chem. Biol. 14, 627–635.
Kim, J.K., Lee, J.R., Kang, J.W., Lee, S.J., Shin, G.C., Yeo, W.S., Kim, K.H., Park, H.S., Kim, K.P., 2011. Anal. Chem. 83, 157–163.
Ko, K.S., Jaipuri, F.A., Pohl, N.L., 2005. J. Am. Chem. Soc. 127, 13162–13163.
Legon, A.C., 2010. Phys. Chem. Chem. Phys. 12, 7736–7747.
Liesener, A., Karst, U., 2005. Anal. Bioanal. Chem. 382, 1451–1464.
López-Otín, C., Hunter, T., 2010. Nat. Rev. Canc. 10, 278–292.
Luo, Y.C., Yan, X.W., Huang, Y.S., Wen, R.B., Li, Z.X., Yang, L.M., Yang, C.Y.J., Wang, Q. Q., 2013. Anal. Chem. 85, 9428–9432.
Ma, R.N., Hu, J.J., Cai, Z.W., Ju, H.X., 2014. Anal. Chem. 86, 8275–8280.
Ma, R.N., Lu, M.H., Ding, L., Ju, H.X., Cai, Z.W., 2013. Chem. Eur J. 19, 102–108.
Meng, X., Hu, J.J., Chao, Z.C., Liu, Y., Ju, H.X., Cheng, Q., 2018. ACS Appl. Mater. Interfaces 10, 1324–1333.
Min, D.H., Su, J., Mrksich, M., 2004. Angew. Chem. Int. Ed. 43, 5973–5977.
Minotti, G., Menna, P., Salvatorelli, E., Cairo, G., Gianni, L., 2004. Pharmacol. Rev. 56, 185–229.
Montavon, T.J., Li, J., Cabrera-Pardo, J.R., Mrksich, M., Kozmin, S.A., 2012. Nat. Chem. 4, 45–51.
Nicholson, R.L., Ladlow, M.L., Spring, D.R., 2007. Chem. Commun. 38, 3906–3908.
Northen, T.R., Lee, J.C., Hoang, L., Raymond, J., Hwang, D.R., Yannone, S.M., Wong, C. H., Siuzdak, G., 2008. Proc. Natl. Acad. Sci. U. S. A. 105, 3678–3683.
O'Kane, P.T., Mrksich, M., 2017. J. Am. Chem. Soc. 139, 10320–10327.
Onagi, J., Komatsu, T., Ichihashi, Y., Kuriki, Y., Kamiya, M., Terai, T., Ueno, T., Hanaoka, K., Matsuzaki, H., Hata, K., Watanabe, T., Nagano, T., Urano, Y., 2017. J. Am. Chem. Soc. 139, 3465–3472.
Percy, A.J., Parker, C.E., Borchers, C.H., 2013. Bioanalysis 5, 2837–2856.
Sanchez-Ruiz, A., Serna, S., Ruiz, N., Martin-Lomas, M., Reichardt, N.C., 2011. Angew. Chem. Int. Ed. 50, 1801–1804.
Vegas, A.J., Bradner, J.E., Tang, W.P., McPherson, O.M., Greenberg, E.F., Koehler, A.N., Schreiber, S.L., 2007. Angew. Chem. Int. Ed. 46, 7960–7964.
Vickers, C.J., Gonzalez-Paez, G.E., Wolan, D.W., 2013a. J. Am. Chem. Soc. 135, 12869–12876.
Vickers, C.J., Gonzalez-Paez, G.E., Wolan, D.W., 2013b. ACS Chem. Biol. 8, 1558–1566.
Xu, X.H., Zhou, J., Liu, X., Nie, Z., Qing, M., Guo, M.L., Yao, S.Z., 2012. Anal. Chem. 84, 4746–4753.
Yang, H., Chan, A.L., LaVallo, V., Cheng, Q., 2016. ACS Appl. Mater. Interfaces 8, 2872–2878.
Yeo, W.S., Min, D.H., Hsieh, R.W., Greene, G.L., Mrksich, M., 2005. Angew. Chem. Int. Ed. 44, 5480–5483.
Yuan, Y.Y., Zhang, C.J., Kwok, R.T.K., Mao, D., Tang, B.Z., Liu, B., 2017. Chem. Sci. 8, 2723–2728.
Zhang, X.B., Liu, C.H., Wang, H.H., Wang, H., Li, Z.P., 2015. Angew. Chem. Int. Ed. 54, 15186–15190.
Zhou, J., Xu, X.H., Liu, X., Li, H., Nie, Z., Qing, M., Huang, Y., Yao, S.Z., 2014. Biosens. Bioelectron. 53, 295–300.